GEOFLUIDS

Geofluids (2013) **13**, 21–31 doi: 10.1111/gfl.12005

Review

Thermal waters of 'tectonic origin': the alkaline, Na-HCO_3 waters of the Rio Valdez geothermal area (Isla Grande de Tierra del Fuego, Argentina)

BRUNO CAPACCIONI[1], MARCO MENICHETTI[2], ALBERTO RENZULLI[2], ALEJANDRO TASSONE[3] AND ANTONIO D. HUERTAS[4]

[1]Department of Earth and Geological-Environmental Sciences, University of Bologna, Piazza Porta San Donato, Bologna, Italy; [2]Department of Earth, Life and Environmental Sciences, University of Urbino "Carlo Bo", Urbino, Italy; [3]CONICET-INGEODAV, Dpto. de Ciencias Geológicas, Facultad de Ciencias Exactas y Naturales, Universidad de Buenos Aires, Ciudad Universitaria, Pabellón 2, CP - C1428EHA- Buenos Aires, Argentina; [4]Laboratorio de Biogeoquímica de Isótopos Estables, Instituto Andaluz de Ciencias de la Tierra IACT(CSIC-UGR), Armilla, Granada, Spain

ABSTRACT

The geothermal area of Rio Valdez is located in the central portion of the Isla Grande de Tierra del Fuego (South Argentina), ten kilometers south of the southeastern sector of the Fagnano Lake. It consists of a series of thermal springs with low discharge rates (≤1 L/s) and temperatures in the range of 20–33°C distributed in an area of <1 km^2. The thermal springs are characterized by alkaline, Na-HCO_3 waters with low salinity (0.53÷0.58 g/L), but relatively high fluoride contents (up to 19.4 mg/L). Their composition is the result of a slow circulation at depth, possibly through deep tectonic discontinuities connected with the Magallanes-Fagnano Fault (MFF) system. According to geothermometric calculations, thermal waters reach temperatures in the range of 100–150°C and an almost complete chemical equilibrium with the alkali-feldspars in the metavolcanic country rocks. The relatively high fluorine contents can be explained by the slow ascent and cooling of deep groundwaters followed by a progressive re-equilibration with F-bearing, hydrated Mg-silicates, such as chlorite, which has been recognized as an abundant mineral in the metavolcanics of the Lemaire Formation and metapelites and metagraywackes of the Yahgán Formation. Finally, the isotopic composition of the investigated samples is consistent with the infiltration from local snow melting at altitudes in the range of 610–770 m asl. The comparison of our data with those collected in 1991 seems to suggest a possible progressive decline of the bulk thermal output in the near future. This possibility should be seriously considered before planning a potentially onerous exploitation of the resource. Presently, the only ways to exploit this geothermal resource by the population scattered in the area are the direct use of thermal waters and/or spa structures.

Key words: Argentina, geochemistry of thermal fluids, geothermal areas, tectonics, Tierra del Fuego.

Received 23 May 2012; accepted 10 October 2012

Corresponding author: Bruno Capaccioni, Department of Earth and Geological-Environmental Sciences, University of Bologna, Piazza Porta San Donato, 1 – 40126 Bologna, Italy.
E-mail: bruno.capaccioni@unibo.it. Tel: +390512094947. Fax: +390512094904.

Geofluids (2013) **13**, 21–31

INTRODUCTION

During the last decade, the development of renewable energy resources has significantly expanded for two main reasons: (i) the steady increase in oil prices and (ii) the impact of greenhouse gases released from combustion of fossil fuels in the atmosphere. Among the available renewable energies, the exploitation of both high- to low-enthalpy geothermal systems (for electric and nonelectric utilizations, respectively) is one of the most promising resources, particularly in Central and Southern America, Western United States, Iceland, New Zealand, Indonesia, the Philippines,

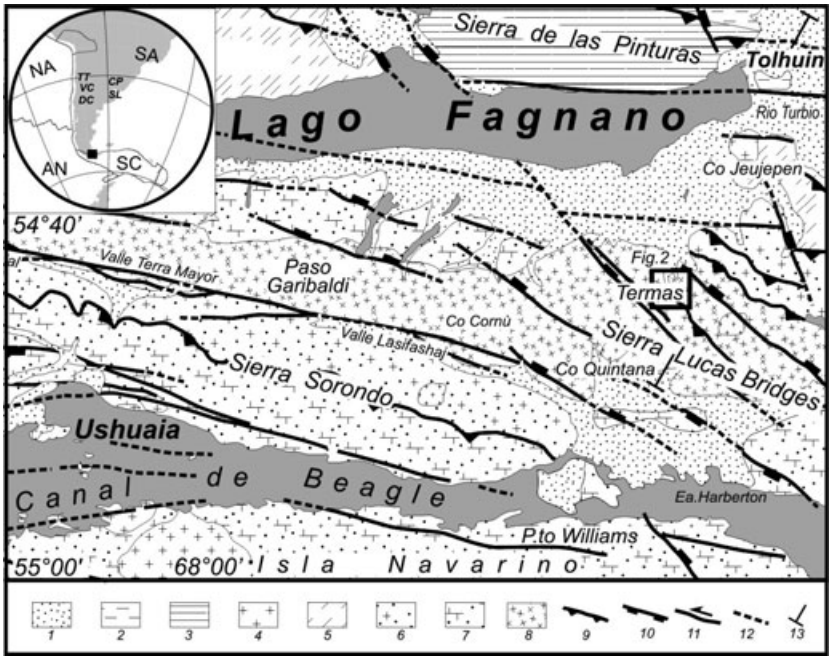

Fig. 1. Geological map of the area south of Fagnano Lake, Tierra del Fuego Island, southernmost sector of South America (small, black square in the upper left inset). A closeup of the Termas of Rio Valdez geothermal area (central right) is shown in Fig. 2. In the upper left inset, a schema of the plate tectonics setting is shown: SA – South America Plate, SC – Scotia Plate, AN – Antarctic Plate, NA – Nazca Plate. Abbreviations of the main ongoing Argentinian geothermal projects are also indicated : CP – low-enthalpy Chaco-Parana Basin; SL- low-enthalpy Salado Basin; TT – high-enthalpy Tuzgle-Tocomar; VC – high-enthalpy Valle del Cura; DC – high-enthalpy Domuyo and Copahue. 1 – Glacial and fluvioglacial sediments (undifferentiated moraine systems and till) and debris, Pleistocene; 2 – Sandstone, marls, and conglomerate with coquina, Rio Claro Group, Lower Paleogene; 3 – Slaty marls, metasandstones, and siltstones, Cerro Matrero Fm., Upper Cretaceous; 4 – Plutonic rocks, syenites, and monzodiorites, Upper Cretaceous; 5 – Dark slates, metamarls, and tuffs, Beauvoir Fm., Lower Cretaceous; 6 – Metasandstones, dark shales, and metatuffs, Yaghan Fm., Lower Cretaceous; 7 – Submarine volcanoclastic metasediments with basalts, Alvear Fm. Auct., Lemaire or Tobifera Fm., Upper Jurassic; 8 – Volcanoclastic metasediments with rhyolites and quartz porphyres, Monte Buckland Fm.Auct., Lemaire or Tobifera Fm., Upper Jurassic; 9 – Thrust fault, triangles in the hanging-wall; 10 – Normal fault, barbs in the hanging-wall; 11 – Strike-slip fault; 12 – Inferred fault; 13 – Trace of the section of Fig. 9.

and Italy (Bertani 2005; Gupta & Roy 2007). In Argentina, based on the results of reconnaissance surveys and geothermal prefeasibility studies of Pesce (1995) and Miranda & Pesce (2000), the volcanic areas of Tuzgle-Tocomar (Salta-Jujuy), Domuyo and Copahue (Neuquén), and Valle del Cura (San Juan) are favorable sites for high-enthalpy projects. As a matter of fact, electricity from high-enthalpy geothermal sources is going to be produced in Copahue, and an evaluation of the potential of this area concluded that production of 30 MW could continue for at least 30 years using the existing steam reservoir located at a depth of approximately 1200 m (Pesce 2010). Several exploitation, development, and prefeasibility projects for direct utilization of the earth's heat (low enthalpy) are located in the Chaco-Parana and Salado Basins (Entre Rios, Santa Fe, Misiones, Buenos Aires, Corrientes and Chaco; Pesce 2005, 2010). Similarly, the Rio Valdez geothermal area (Isla Grande de Tierra del Fuego; Fig. 1) presents good prospects for the direct exploitation (nonelectric) of low-temperature waters (Pesce & Pedro 1995).

The Rio Valdez geothermal area is located 60 km east–northeast of Ushuaia (Fig. 1) and is characterized by a tundra climate with an average annual temperature and rainfall of 5°C and 800 mm/y, respectively. As a result of these climatic conditions, small glacial cirques and permanent snow patches are widespread at elevations of 800–1000 m asl. The present use of the low-temperature waters of the Rio Valdez is restricted to bathing and relaxation in an uncontaminated environment. The preliminary study performed by Pesce & Pedro (1995) on the Rio Valdez thermal waters is the only available geochemical investigation of the area. They describe sodium-bicarbonate compositions on samples collected in 1991 with an average temperature of 38.5°C, a pH range of 7.8–8.2, and a conductivity between 613 and 658 μs/cm. The authors also report the presence of free gases at the emergence points, whose occurrence has not been confirmed during the sampling campaign carried out in 2009 (present work). Although no $\delta^{18}O_{H2O}$ and δD_{H2O} data have been reported, the highest areas of the Fuegina Cordillera were identified as the recharge areas and, based on the absence of Tritium, a residence time <20 years was estimated, with a water/rock equilibration attained in the deep metamorphic basement at temperature conditions

between 88 and 98°C (according to various geothermometers).

The only significant urban settlements located in this sector of the Isla Grande de Tierra del Fuego are Ushuaia and Tolhuin (Fig. 1). Most of the remaining population is scattered in many small rural estates ('*estancias*'). This makes the Rio Valdez geothermal area a potential diffuse heat resource for local energy supply.

In order to verify the potential of further exploitation of this natural resource, this paper presents a detailed characterization of the Rio Valdez thermal waters using a geochemical approach integrated with geological and structural data.

STRUCTURAL GEOLOGY AND GEOMORPHOLOGY

The Fuegina Cordillera represents the southernmost part of the Andes. Its evolution began in the Mesozoic–Cenozoic with Middle to Late Jurassic back-arc extension related to the break-up of Gondwanaland (Dalziel & Elliot 1973; Dalziel & Brown 1989; Menichetti *et al.* 2008 and reference therein). This part of the Andes records the Meso-Cenozoic tectono-sedimentary events related to the development of the extensional Rocas Verdes back-arc basin (Katz 1972), the compressional phase with the formation of the Magallanes foreland basin (Biddle *et al.* 1986), and finally the wrench tectonics with the generation of pull-apart basins (Lodolo *et al.* 2003). The oldest rocks of the Fuegina Cordillera, representing the pristine metamorphic basement of the chain, consist of polydeformed, medium- to high-grade metasedimentary, and metavolcanic rocks belonging to the garnet-amphibolite facies. They crop out on the western flank of the Cordillera (Cordillera Darwin), an elongated relief with an average altitude of 2000 m (Nelson *et al.* 1988). In this framework, the Rio Valdez thermal basin rests on the northern foothills of the Fuegina Cordillera in an area characterized by the Magallanes foreland fold and thrusts belt consisting of a NNE imbricate system of thrust duplexes developed during the Paleocene–Oligocene, with a thin-skinned tectonic style involving a Cenozoic silicoclastic syntectonic foredeep wedge (Tassone *et al.* 2005; Menichetti *et al.* 2008). Based on unconformities within the Paleogene syntectonic stratigraphic succession (which during the Quaternary glacial events are locally sealed by a thick continental succession of fluvial, lacustrine and glacial sedimentary facies; Rabassa *et al.* 1989) the timing of thrust propagation through the foreland basin points to at least three deformation events (Menichetti & Tassone 2007; Menichetti *et al.* 2008).

The Rio Valdez consists of a N-S-oriented glaciofluvial valley covered by deciduous forest and shrubs, peat-bog mires, and grassland. It drains a hydrographic basin of about 60 km^2 with a maximum altitude of 800 m asl (Co Chechen high). The river is one of the most important tributaries of the Fagnano Lake and is fed by several small glacial lakes and springs located in the mountain area. It moves, initially, in a N-S direction, turning toward the NE in the zone of thermal springs where it is joined by a small, unnamed tributary on the eastern bank (Fig. 2). The

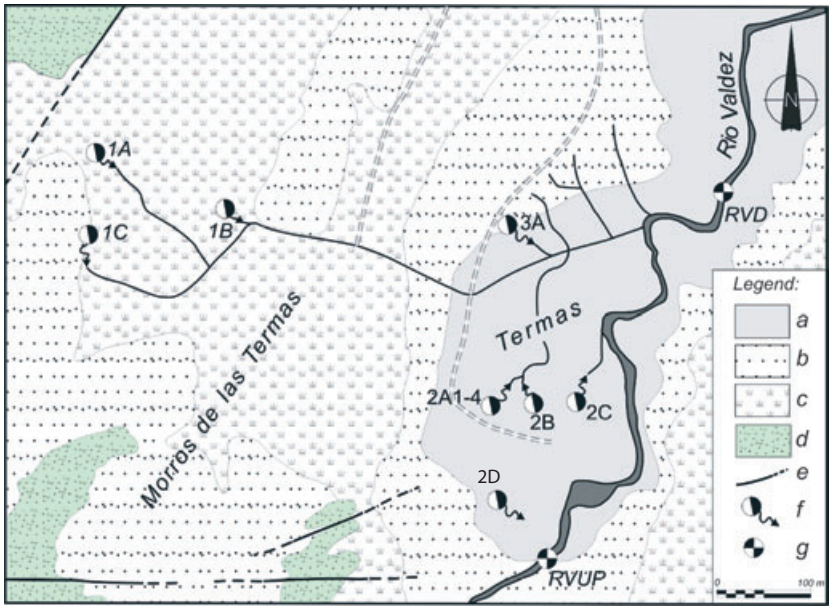

Fig. 2. Schematic map of the Termas of the Rio Valdez geothermal area. Legend: a: The Termas area; b: Area covered by forest; c: Area covered by peat-bogs; d: Outcrop of the Lemaire Fm.; e: Fault and inferred fault; f: Main pools (with water sample locations) and inferred streams (arrows); g: Locations of the upper (RVUP) and lower (RVD) Rio Valdez water samples. Location map in Fig. 1.

glaciofluvial deposits of the talweg are lightly carved by several meanders. The present morphology, characterized by the occurrence of several isolated drumlins along the eastern bank of the Rio Valdez, is mostly the result of Quaternary glacial processes. North of the thermal area, glacial deposits, with a thickness of about one hundred meters but increasing progressively toward the Fagnano Lake, fill the Rio Valdez valley.

The thermal springs are located on the northern slope of the Sierra Lucas Bridge, along the western bank of the Rio Valdez valley (Figs. 1 and 2). They are distributed in two different areas (Fig. 2): on the left-hand side of Rio Valdez at 200 m asl and ~600 m westward on a terrace covered by large peat-bogs at 250 m asl.

GEOLOGICAL FORMATIONS AND PETROGRAPHY

Surface geology of the study area is mainly represented by metarhyolite to metarhyodacite lavas and ignimbrites, metatuffs, metabreccias, metatuffaceous turbidites, and slates of Middle to Late Jurassic, pertaining to the Lemaire Formation (Tobífera Formation, in the neighboring Chile) (Fig. 1). The magmatism of the Lemaire Formation is interpreted as the result of widespread melting of the continental crust (Pankhurst *et al.* 2000 and references therein) due to regional extension associated with the break-up of Gondwana in the Lower to Middle Jurassic (Bruhn 1979). In areas surrounding the Rio Valdez thermal basin, the Lemaire Formation is represented by felsic metavolcanics (rhyolites to dacites), of a minimum thickness of 150 m, which are strongly affected by mineral replacement and characterized by the presence of low- to medium-grade metamorphic minerals such as epidote, sericite, and chlorite (Pesce & Pedro 1995). The extensional period, which gave rise to the Lemaire Formation, was also associated with the formation of oceanic crust during the development of the Rocas Verdes marginal basin and the consequent deposition of a marine sequence known as the Yahgán Formation (Dalziel 1981; Olivero & Martinioni 2001). The latter is a regionally metamorphosed marine sequence dating back to Upper Jurassic–Lower Cretaceous (Caminos *et al.* 1981), consisting of metapelites and metagraywackes and outcropping mainly south of the Río Valdez thermal basin. The sedimentary filling of the Upper Jurassic Rocas Verdes Basin, north of the studied area, is represented by the Beauvoir Formation (Camacho 1967), which consists of dark slates and gray tuffs with scarce rhythmites of sandstones and mudstones. The geological units related to the extensional event of the Rocas Verdes Basin (i.e., Lemaire, Yahgán, and Beauvoir formations) host Late Cretaceous intrusions characterized by a distinct shoshonitic nature (Cerredo *et al.* 2000). The Fuegian plutons show a large compositional span from ultramafic (pyroxenites–hornblendites) through monzogabbros–monzodiorites–monzonites to syenite facies (Cerredo *et al.* 2005, 2007; Peroni *et al.* 2009; González Guillot *et al.* 2009). The Cerro Jeujepén (CJJ) intrusion (Fig. 1), a small (<10 km^2) Late Cretaceous (93 ± 4 Ma) magmatic body stretching along the inferred strike of the Magallanes-Fagnano Fault (MFF) system at the SE tip of Fagnano Lake (Cerredo *et al.* 2005), is the nearest intrusive body to the Rio Valdez area where magnetic and gravimetric data have also suggested the existence of a prominent crystalline body in the subsurface (roots at depth of about 8 km; Cerredo *et al.* 2000). The CJJ intrusion is a composite plug mostly composed of intermediate rocks (monzodiorite, monzonite, and syenite) with SiO_2-undersaturated compositions (nepheline normative) and a clear shoshonitic affinity (Cerredo *et al.* 2000, 2005; Ridolfi *et al.* 2010). Other extensive shoshonitic intrusive bodies related to the Fuegian Potassic Magmatism crop out 50 km to the southeast of the Rio Valdez area (Moat Dioritic Pluton; González Guillot *et al.* 2009). These alkaline intrusions and related metapelite and metagraywacke, wall rocks of the Yahgán Formation may have played a fundamental role in determining the composition of the Rio Valdez thermal waters.

SAMPLING AND ANALYTICAL METHODS

Eight thermal water samples from hot pools (1A, 1B, 1C, 2A1, 2A4, 2B, 2C, 2D; Fig. 2), two cold river water samples from the Rio Valdez river (up- and down-current with respect to the thermal field, RVUP and RVD; Fig. 2), and one cold water spring sample (3A; Fig. 2) were collected and analyzed for major and minor chemical constituents, $\delta^{18}O_{H2O}$ and δD_{H2O} (Fig. 2; Tables 1 and 2). Two rain samples (A–B, collected at Tolhuin and Ushuaia, respectively), and two snow ones, (C-D, collected at Rio Valdez and Paso Garibaldi, respectively), were only analyzed for $\delta^{18}O_{H2O}$ and δD_{H2O} (Table 2). All water isotopes were analyzed at the Laboratorio de Biogeoquímica de Isótopos Estables of the Instituto Andaluz de Ciencias de la Tierra (Granada, Spain). Temperature and pH values were measured *in situ*. Chemical analyses were carried out by molecular spectrophotometry (MS, Hach DR2010) for NH_4^+, acidimetric titration (with 0.01 N HCl) for alkalinity, ion chromatography (IC, Dionex ICS 90) for F^-, Cl^-, Br^-, NO_3^-, and SO_4^{2-}, atomic absorption spectrophotometry (AAS, Perkin-Elmer AAnalyst 100) for Na^+, K^+, Ca^{2+}, Mg^{2+} and Li^+, and inductively coupled plasma atomic emission spectrometry (ICP-AES, Thermo iCAP 6000) for SiO_2 and H_3BO_3. The analytical errors for IC, AAS, and ICP-AES were ≤5%. Analytical data are reported in Table 1.

The $^{18}O/^{16}O$ and $^{2}H/^{1}H$ isotopic ratios (expressed as $\delta^{18}O‰$ and $\delta D‰$ V-SMOW) in water samples were determined using a Finnigan Delta Plus XL mass spectrometer following standard protocols. Oxygen isotopes were analyzed using the CO_2–H_2O equilibration method proposed

Table 1 Chemical compositions and TDS (total dissolved solids) of thermal and cold water samples collected in the Rio Valdez geothermal area. Concentrations expressed as mg/L.

Sample	Sample description	Date of sampling	T°C	pH	Eh mV	Na^+	K^+	Ca^{2+}	Mg^{2+}	HCO_3^-	CO_3^{2-}	F^-	Cl^-	NO_3^-	SO_4^{2-}	Li^+	NH_4^+	H_3BO_3	Rb^+	Cs^+	SiO_2	TDS g/L	$SI_{calcite}$	$SI_{fluorite}$
1A	Thermal spring	Nov-09	33.1	7.95	−52	171	4.6	4.5	0.24	342	bdl	16.50	25.1	1.3	7.5	0.87	0.12	6.1	0.01	bdl	36.38	0.57	−0.21	0.06
1B	Thermal spring	Nov-09	20.4	8.53	−49	156	4	5	0.17	335	24	17.40	25.6	0.2	5.9	0.91	0.11	6.1	bdl	bdl	37.45	0.57	0.63	0.28
1C	Thermal spring	Nov-09	24.5	8.26	−58	155	4.3	6.4	0.2	300	12	16.70	25.9	0.3	5.6	0.87	0.13	6.0	0.01	2	36.59	0.53	0.47	0.31
2A1	Thermal spring	Nov-09	29.8	8.20	−45	153	4.4	5.4	0.29	323	18	16.80	25.3	0.5	5.8	0.88	0.11	6.4	bdl	1	34.67	0.55	0.56	0.15
2A4	Thermal spring	Nov-09	33.5	8.20	−46	152	3.9	5.2	0.22	317	18	16.80	27.8	1.5	4.8	0.9	0.12	6.2	bdl	bdl	34.45	0.55	0.57	0.11
2B	Thermal spring	Nov-09	28.7	8.50	−42	152	3.9	5.3	0.27	332	18	17.25	26.5	0	6.4	0.89	0.07	5.8	0.01	bdl	35.74	0.56	0.56	0.21
2C	Thermal spring	Nov-09	30.3	8.45	−42	160	3.8	5.6	0.27	345	9	19.40	30.9	0.5	6.8	0.83	0.08	5.9	bdl	bdl	35.52	0.58	0.29	0.32
2D	Thermal spring	Nov-09	27.0	8.13	−48	152	4.1	5.4	0.22	354	bdl	16.60	25.1	1.3	7.4	0.88	0.14	6.1	bdl	bdl	35.52	0.57	−0.01	0.23
3A	Cold spring	Nov-09	8.6	7.04	37	10	0.6	5.9	2.53	36	bdl	0.10	9.6	3	3	bdl	bdl	1.2	bdl	bdl	14.55	0.07	−2.20	−3.93
RVUP	River water upcurrent	Nov-09	7.9	7.84	50	3	0.2	5	0.83	15	bdl	0.07	3.1	0.9	6.6	bdl	0.02	0.9	bdl	bdl	3.42	0.03	−1.77	−4.24
RVD	River water downcurrent	Nov-09	8.3	7.64	48	10	0.2	4.2	0.78	30	bdl	0.25	3.2	0.8	6.2	bdl	bdl	0.5	bdl	bdl	3.64	0.06	−1.77	−3.24

Table 2 Temperatures calculated according to Na/K, K^2/Mg, and silica geothermometers for thermal waters collected in the Rio Valdez geothermal area.

Sample	T°C Na/K (Fournier 1979)	T°C Na/K (Giggenbach 1988)	T°C K^2/Mg (Giggenbach 1988)	T°C SiO_2 (Fournier 1991)
1A	125	145	93	88
1B	123	143	94	89
1C	127	147	93	88
2A1	129	149	89	85
2A4	123	143	90	85
2B	123	143	87	87
2C	119	139	86	87
2D	126	146	91	87

by Epstein & Mayeda (1953). Hydrogen isotopic ratios of H_2 were measured after the reaction of 10 mL of water with metallic zinc at 500°C. The experimental errors for $\delta^{18}O$ and δD_{H2O} were ±0.1 and ±1‰, respectively, as calculated using EEZ-3 and EEZ-4 as internal standards previously calibrated versus V-SMOW and SLAP reference standards.

HYDROCHEMISTRY AND DISCHARGE RATE OF THERMAL WATERS

The Rio Valdez thermal waters, collected in November 2009, are characterized by temperatures in the range of 20–33°C, pH values of 8–8.5, low salinities, and TDS (total dissolved solids) not exceeding 0.58 g/L (Table 1). Average temperature and pH significantly differ from those reported by Pesce & Pedro (1995) for samples collected in 1991. Temperature is about 10°C lower (28.4 vs 38.5°C), while pH is slightly higher (8.3 vs 7.8–8.2). As reported below, these differences appear to be also associated with a significant lowering of the 'bulk' discharge rate (13.8 vs 18 L/s). According to the square classification diagram (Fig. 3; Langelier & Ludwig 1942), the eight thermal waters display quite homogeneous Na-HCO_3 compositions, while the Rio Valdez (RVUP and RVD) waters and the cold spring (3A), with temperatures ~8°C, appear to be arranged from very diluted Ca-HCO_3 to Na-HCO_3 water types, revealing different degrees of binary mixing between the two. Therefore, while the homogeneous composition of thermal waters suggests a negligible mixing with shallow groundwaters before their emergence, the highly diluted river water (total dissolved solids – TDS = 0.07 g/L) collected downcurrent seems to be significantly contaminated by thermal waters.

Concerning the minor components (Table 1), thermal waters are characterized by relatively high concentrations of F^- (16.4–19.4 mg/L; Table 1) and H_3BO_3 (5.8–6.4 mg/L); minor concentration of NH_4^+ (0.08-0.14 mg/L), NO_3^- (0.2–1.3 mg/L), and Li^+ (0.83–0.91 mg/L);

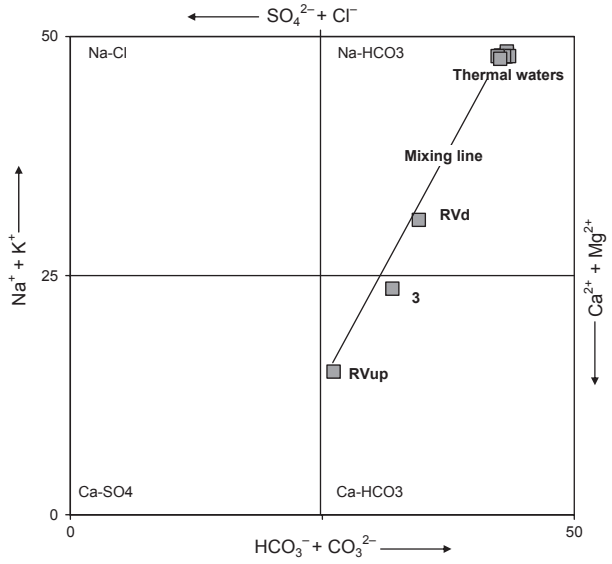

Fig. 3. Square classification diagram (Langelier & Ludwig 1942) for the thermal and cold waters collected in the Rio Valdez geothermal area.

and traces of Rb^+ and Cs^+. Despite the relatively low Ca^{2+} concentrations (Table 1), with the exception of 1A and 2D, they range from calcite- and fluorite-saturated to slightly over-saturated ($-0.21 < SI_{calcite} < 0.63$ and $0.06 < SI_{fluorite} < 0.32$, where SI is the Saturation Index = log IAP/K_{sp}, calculated using the PHREEEQC code, version 2.15.0, Parkhurst 1995).

According to the conservative behavior of F^- and Na^+ in the diluted river waters ($SI_{fluorite} < -1$) and giving their contents in water samples collected upstream and downstream with respect to the main thermal area (2A-D pools), we can apply the following mass balance calculation:

$$C_d = C_{up}x_{up} + C_t x_t \quad (1)$$

where:

$$x_{up} + x_t = 1 \quad (2)$$

where C_d is the concentration of the conservative components in the downstream waters (0.25 and 10 mg/L, respectively, RVD sample, the mixing term), C_{up} the concentration of the same components in the upstream water (0.07 and 3 mg/L, respectively, RVUP sample), C_t their concentration into the thermal water (17.4 and 156 mg/L, respectively, 1B sample), and x_{up} and x_t are the fraction of the upstream and thermal water into the downstream water (mixing term), respectively.

By combining equations (1) and (2),

$$x_t = (C_d - C_{up})/(C_t - C_{up}) \quad (3)$$

Ifwe substitute the measured concentrations, we obtain $x_t = 0.01$ for F^- and $x_t = 0.046$ for Na^+. This significant difference could be related to nonconservative behavior of F^-, which could have been precipitated as CaF_2 before the mixing with the river water. Therefore, according to the Na^+ contents, the variation in the downstream water composition can be explained by the input of ~4.6% of thermal water. By considering the measured discharge rate of Rio Valdez (~300 L/s measured at the RVD site; Fig. 2), this calculated fraction allows estimation of a direct thermal water discharge into the river of ~13.8 L/s (49.7 m^3/h). This 'bulk' value is larger than the sum of the discharge rates directly measured at each thermal pool (23 m^3/h), but lower than the 18 L/s (64.8 m^3/h) estimated by Pesce & Pedro (1995).

WATER–ROCK EQUILIBRIA AND GEOTHERMOMETRY

As already pointed out by Marini *et al.* (2000), alkaline Na-HCO_3 waters, where not related to ion-exchange phenomena (Capaccioni *et al.* 2005), usually represent 'mature' waters, that is, water solutions whose composition is fully equilibrated with rock minerals (carbonates and silicates) at the temperature and pressure conditions prevailing at depth (Giggenbach 1988). Their chemical compositions, the moderate thermal characteristics, and the low discharge rates were attributed to long-lasting water–rock interactions, which occur in slow-moving groundwaters, usually rising along fault systems. According to the calcite-saturation diagram reported in Fig. 4, while the calcite-unsaturated Ca-HCO_3 cold waters plot close to the expected $[Ca^{2+}]/[HCO_3^-]$ ratio for a multiphase reaction with

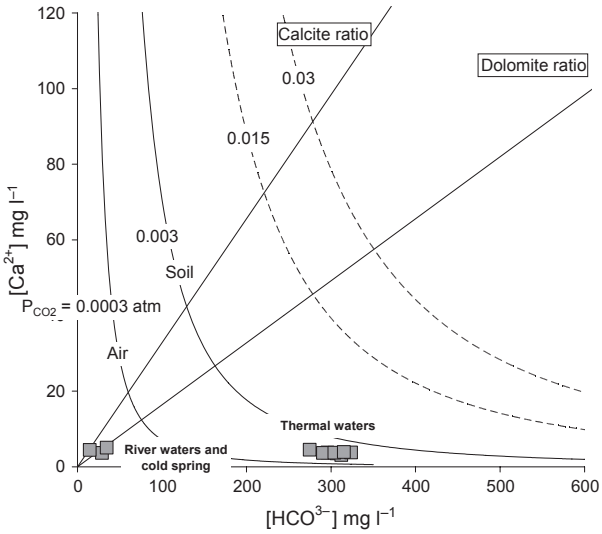

Fig. 4. $[HCO_3^-]$ vs. $[Ca^{2+}]$ (mg/L) binary diagram for the thermal and cold water samples collected in the Rio Valdez geothermal area. Solid line represents the $[HCO_3]/[Ca^{2+}]$ values expected for calcite and dolomite dissolution based on a heterogeneous equilibrium: $CaMg(CO_3)_2 + 2CO_2 + 2H_2O = Ca^{2+} + Mg^{2+} + 4HCO_3^-$. Solid curves represent equilibrium conditions at different P_{CO2}.

Ca- and Ca-Mg-carbonates, the compositions of calcite-saturated thermal waters display a large [Ca^{2+}] deficiency compared to [HCO_3^-]. Therefore, ruling out any selective extraction of Ca^{2+} due to calcite precipitation, which should also involve the carbonate ionic species, a reasonable explanation would be the existence of an additional CO_2 source, distinct and independent of the contribution from hydrolysis of solid carbonates. This feature, together with the observed negative Eh values (Table 1), is recurrent for alkaline, Na-HCO_3 thermal waters, as it has already been observed in the Apennine orogen (Central Italy) and in other active tectonic contexts (Marini *et al.* 2000). External inputs of CO_2 can be related to surficial addition due to the oxidation of organic soil matter and/or the rising of CO_2-dominated fluids along deep fault systems. While only the measurements of $\delta^{13}C_{TDIC}$ could be enlightening about these two hypotheses, the scarce interaction of thermal waters with shallow aquifers seems to rule out the former one. Therefore, inputs of dry, CO_2-dominated gas mixtures from depth could be responsible for the observed CO_2 excess, but not for the H_3BO_3 relative enrichment (Table 1), due to its preferred fractionation into the vapor phase only at temperatures >250–300°C. Moreover, as reported by Marini *et al.* (2000), the extremely long residence time of Na-HCO_3 waters at depth results in very low Eh conditions, as also testified by the significant occurrence of NH_4^+ (0.10–0.14 mg/L; Table 1).

The extent of the water–silicate interactions is well illustrated by the log[K^+]/[H^+] vs log[Na^+]/[H^+] activity plots for alkali-feldspars and their alteration products at 30, 90, and 150°C and 1–5 bar (Fig. 5). The activity ratios of the Rio Valdez thermal waters plot within the muscovite field, at 30°C and 1 bar, and show a very good fit with the invariant point of final equilibrium between K-feldspar, albite, muscovite, and the aqueous solution at 150°C and 5 bar.

The possible existence of water–mineral equilibria allows us to apply geothermometric calculations based on ionic solutes geothermometers. Table 2 reports the calculated temperatures according to silica (quartz solubility), Na/K, and K^2/Mg ionic solute geothermometers (Fournier 1979, 1991; Giggenbach 1988). As already inferred from Fig. 5, thermal waters display Na/K equilibrium temperatures in the range of 120–150°C, well above the measured values (20–33°C), suggesting that the compositions of the thermal waters are consistent with the attainment of a water–mineral equilibrium involving alkali-feldspars during circulation at depth. This is in agreement with the slow kinetics of the Na/K exchange between alkali-feldspars and aqueous solutions below 300°C as indicated by both experiments (Orville 1963; Hemley 1967) and well discharge analyses. Re-equilibration, as reflected by the Na/K ratio, usually proceeds slower than predicted by the quartz

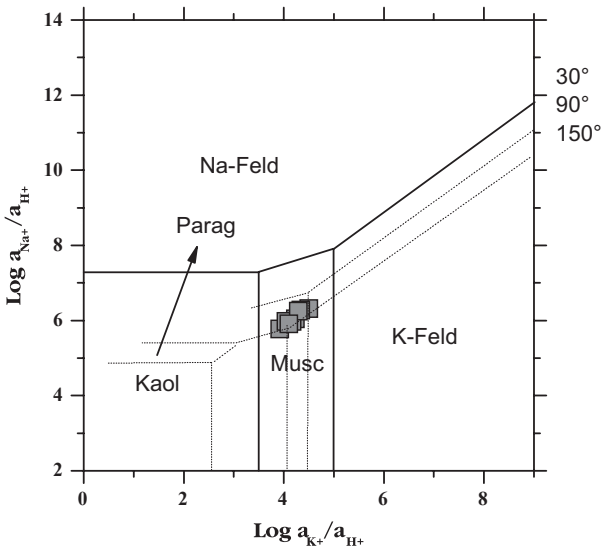

Fig. 5. Log(aNa^+/aH^+) vs log(aK^+/aH^+) activity diagram for the thermal and cold water samples collected in the Rio Valdez geothermal area showing the stability fields for alkali-feldspars, muscovite, kaolinite, and paragonite at different *T*(°C) conditions.

solubility geothermometer (Fournier 1991), as testified by calculated temperatures in the range of 87–89°C.

Due to the re-equilibration of the waters with chlorites or other Mg-bearing minerals (e.g., montmorillonites and saponites), Ellis (1971) recognized that Mg contents of thermal waters are also strongly temperature dependent. Giggenbach (1988) suggested that the K/Mg system approaches mineral–solution equilibrium at temperatures as low as 25°C. This implies relatively fast kinetics of this water–mineral system, even at relatively low temperatures. As expected, the calculated temperature of the Rio Valdez thermal waters according to the K^2/Mg geothermometer (Table 2) is in the range of 86–94°C, which is significantly lower with respect to values calculated using the Na/K activity ratio and mostly in agreement with those obtained with the kinetically faster quartz geothermometer. As stated above, surficial inputs of Mg due to the addition of shallow waters can be ruled out because of the absence of the mixing effects on thermal waters at shallow levels. Moreover, the involvement of hydrated Mg-silicates in the water/rock re-equilibration processes during cooling appears to be consistent with the observed inverse correlation between F^- and $T_{K2/Mg}$ (Fig. 6). The fluorine increase with decreasing temperature of the equilibrium involving magnesium is in good agreement with both Mg- and F-release from chlorite or other hydrated silicate/phyllosilicates of metamorphic rocks in which significant amounts of F^- replace hydroxyl ions. Similarly, F^- enrichment can be the result of interaction with alkaline (potassic) igneous rocks, which normally contain more haloids than any other magmatic series (Müller & Groves 1993). According to

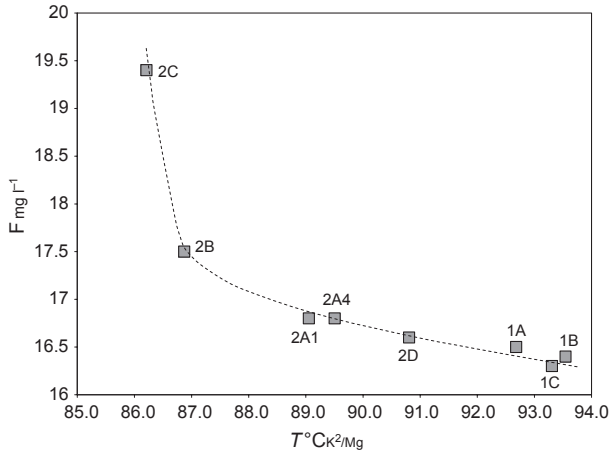

Fig. 6. Binary plot of F^- vs *T*°C (calculated with the K^2/Mg geothermometer) for the thermal water samples collected in the Rio Valdez geothermal area. The sample names are indicated.

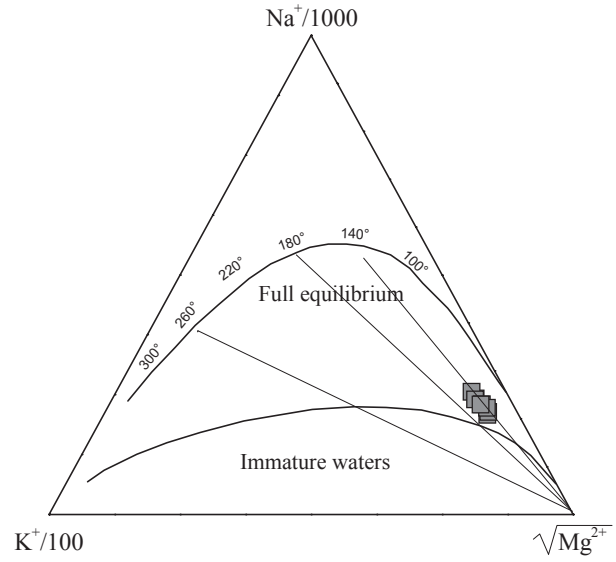

Fig. 7. The $Na/K/Mg^{1/2}$ triangular plot for the thermal water samples collected in the Rio Valdez geothermal area combining the fast-responding K/Mg geothermometer with the slowly re-equilibrating Na/K geothermometer (Giggenbach 1988).

Table 2 and Fig. 6, samples collected ~600 m westward of the Rio Valdez, in a terrace covered by large peat-bogs at an altitude of 250 m asl (sample 1A–C), display a moderate-to-higher $T_{K2/Mg}$ and T_{SiO2} and lower F^- compared to the samples collected on the left-hand side of the Rio Valdez river at an altitude of 200 m asl (sample 2 A–D). Given the similar $T_{Na/K}$ among the two sample groups, we argue that the differences could be related to a faster ascent rate and therefore a lower degree of re-equilibration with Mg-bearing minerals and silica of one group of water samples with respect to the other.

Finally, the triangular plot in Fig. 7, taken from Giggenbach (1988), represents the possibility of the attainment of full or partial water–rock equilibrium by combining the Na/K and K^2/Mg ionic solute geothermometers. The Rio Valdez samples plot in the partial equilibrium zone and are evenly distributed along a line radiating from the $Mg^{1/2}$ vertex (constant Na/K), indicating quasi-constant Na/K and more variable $K/Mg^{1/2}$ equilibrium temperatures. This suggests the attainment of water–mineral equilibrium with alkali-feldspars at depth followed by variable Mg released from Mg- and F-bearing minerals during ascent and cooling.

ISOTOPE GEOCHEMISTRY

The isotopic compositions of the thermal water samples, as well as the isotopic compositions of meteoric water and snow samples collected at different elevations (Table 3), are reported in the δD–$\delta^{18}O$ diagram of Fig. 8. The sample points appear to be well distributed along the Global Meteoric Water Line (GMWL; Craig 1963). The observed isotopic differences between the two meteoric water samples largely exceed the expected range for their different elevation (Poage & Chamberlain 2001). Despite the fact that the two meteoric water samples were collected within a couple of days, the large differences in the isotopic composition may be related to the different provenance of the air masses. The comparison of river and thermal waters, emerging at 200 ÷ 250 m asl, with rainfall samples collected at lower elevations (10 ÷ 120 m asl), shows that their isotopic compositions are too heavy to be consistent with a direct recharge by precipitation in liquid form. As reported on Table 3, snow samples display isotopic compositions significantly heavier than meteoric waters, possibly because of the isotopic fractionation due to sublimation effects (Lechler & Niemi 2011). At the same time, the $\delta^{18}O‰$ values of thermal waters are lighter than those of the snow samples collected at Paso Garibaldi (450 m a.s.l.) and along the Rio Valdez valley (283 m a.s.l.). Therefore, we can conclude that the recharge for the thermal waters is more reasonably associated with snow melting followed by infiltration than direct infiltration of meteoric waters. Assuming a linear correlation between elevation and isotopic composition of snow, the elevation of the recharge area could be in the range of 610–770 m a.s.l., ~500 m higher than the emergence points of thermal springs.

The distribution of the isotopic compositions confirms the meteoric origin of the thermal waters the lack of any ^{18}O-shifting is consistent with temperatures at depth lower than 150°C (Truesdell & Hulston 1980).

THE CONCEPTUAL MODEL

According to stable isotope data, the thermal waters from Rio Valdez area are fed by local snowmelt infiltration at an elevation range of 610–770 m asl. Their alkaline pH and

Table 3 Isotopic compositions of meteoric, thermal, and cold water samples collected in the Rio Valdez geothermal area and other localities indicated in Fig. 1.

Sample	Sample description	Date of sampling	δD (V-SMOW)	$\delta^{18}O$ (V-SMOW)
1A	Thermal spring	Nov-09	−81.24	−10.86
1B	Thermal spring	Nov-09	−81.14	−10.45
1C	Thermal spring	Nov-09	−84.25	−11.44
2A1	Thermal spring	Nov-09	−83.94	−11.32
2A4	Thermal spring	Nov-09	−83.28	−11.04
2B	Thermal spring	Nov-09	−85.69	−11.44
2C	Thermal spring	Nov-09	−81.75	−10.76
2D	Thermal spring	Nov-09	−84.56	−11.09
3A	Cold spring	Nov-09	−71.09	−9.70
RVUP	River water upcurrent	Nov-09	−74.15	−10.34
RVD	River water downcurrent	Nov-09	−72.25	−10.62
A	Rain at Tolhuin 120 m	Nov-09	−119.09	−15.49
B	Rain at Ushuaia 0 m	Nov-09	−63.99	−8.56
C	Snow at Rio Valdez 283 m	Nov-09	−41.10	−7.16
D	Snow at P.Garibaldi 450 m	Nov-09	−56.42	−8.30

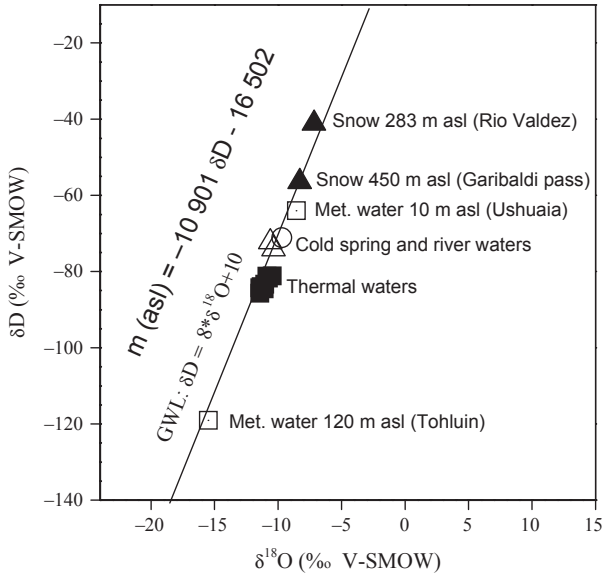

Fig. 8. $-\delta^{18}O_{V\text{-}SMOW}$ vs. $\delta D_{V\text{-}SMOW}$ binary diagram for the thermal and cold water samples collected in the Rio Valdez geothermal area. The solid line represents the Global Meteoric Water Line (GWL in the figure) (Craig 1963). Legend: black triangle – snow at the Rio Valdez (C, altitude 283 m asl) and Paso Garibaldi (D, altitude 450 m asl); open square – meteoric water at Ushuaia (B, altitude 10 m asl) and Tolhuin (A, altitude 120 m asl); open circle – cold spring; open triangle – river waters; black square – thermal waters.

Na-HCO_3 compositions are consistent with a long-lasting water–rock interaction, which implies an almost complete equilibration with alkali-feldspars followed by a partial re-equilibration with hydrated Mg-silicate/phyllosilicates during ascent and cooling. The geological cross-section reported in Fig. 9 displays likely groundwater flow patterns mostly driven through the discontinuous tectonic structures bordering the Magallanes-Fagnano Fault system. Waters infiltrating at an altitude of ~700 m slowly migrate downwards along the fractured zone of the tectonic discontinuities (normal fault system) possibly reaching as deep as 5–6 km (Menichetti *et al.* 2008). At this point, due to the hydrostatic load, confined groundwaters are able to move along subhorizontal thrusts and inverse faults systems ascending and emerging when the next, parallel, subvertical normal fault is intercepted. The possible maximum temperature of ~150°C reached along the water's flowpath implies a 'normal' geothermal gradient of 25–30°C/km (Rossello *et al.* 2008). By combining the inferred flow length of the thermal groundwaters and their minimum residence time at depth of 20 year (as inferred by the lack of measurable TU; Pesce & Pedro 1995), a mean saturated hydraulic conductivity in the range of 10^{-5}–10^{-4} m/s can be empirically calculated, which is largely consistent with the expected values for fractured rocks (Shapiro & Hsieh 1998). A slow ascent can not only justify the measured low discharge rate and thermal re-equilibration, but also explain the progressive re-equilibration of waters with hydrated Mg-silicates and quartz, increasing the pH, as well as the Mg^{2+} and F^- contents. The water–mineral system reaches equilibrium conditions at 80–90°C. This interpretative model is largely consistent with a slow leaching of cretaceous alkaline intrusions (Fuegian Potassic Magmatism) at a depth of approximately 5–6 km possibly followed by re-equilibration with the chlorite-bearing rocks of the Yahgán and Lemaire Formation as the waters rise and cool.

CONCLUSIONS

The thermal springs in the Rio Valdez basin can be associated with the existence of a deep, subvertical fault system and thrusts connected with the Magallanes-Fagnano Fault

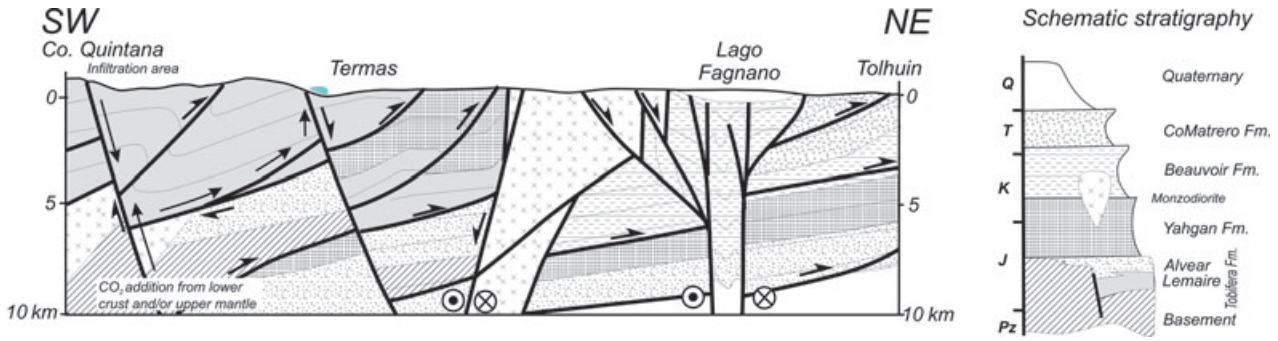

Fig. 9. Schematic stratigraphy and N-S cross-section for the Rio Valdez geothermal area (inferred from field geology and seismic data). The infiltration area and the hydrological flow path of the thermal water are also indicated. Location of the cross-section is shown in Fig. 1.

(MFF) system. They represent the emergence of slow-moving, deep groundwaters whose chemical and isotopic compositions suggest the achievement of an almost full chemical equilibrium at depth in the range of 100–150°C. At this depth, further chemical and thermal contributions from fluids rising from the lower crust and/or upper mantle can be hypothesized. Our data significantly differ from those reported by Pesce & Pedro (1995) on samples collected in 1991. Generally speaking, these differences seem to be driven by a significant lowering of the bulk discharge rate. This, in turn, could be responsible for the more efficient cooling of thermal waters, loss of dissolved CO_2, and increase in pH before emerging at the surface.

Although in the near future a possible progressive decline of the bulk thermal output cannot be ruled out, the Rio Valdez thermal area is presently suitable for direct geothermal use, that is, spa structure and/or thermal energy production through heat exchange.

ACKNOWLEDGEMENTS

The authors are grateful to two anonymous reviewers for their helpful criticism and Rosanna Cozzolino for her language revision, as well as the people that have, in various ways, contributed to the field work in Tierra del Fuego and, in particular, to José Luis Hormaechea and Gerardo Connon of the Estación Astronómica Río Grande EARG - Universidad Nacional de La Plata Argentina. This study was financially supported by CUIA (Consorzio Universitario Italiano per l'Argentina) through the 'Geotermia a bassa entalpia in Tierra del Fuego' project (scientific coordination of M.M; third call for proposals of CUIA projects, 2008–2009).

REFERENCES

Bertani R (2005) World geothermal power generation in the period 2001-2005. *Geothermics*, **34**, 651–90.

Biddle KT, Uliana MA, Mitchum RM, Fitzgerald MG, Wright RC (1986). The stratigraphic and structural evolution of the central and eastern Magallanes basin, southern South America. In: Allen PA, Homewood P (Eds.), Foreland Basins: Int. Assoc. Sediment. Spec. Publ., vol. 8, pp. 41–61.

Bruhn RL (1979) Rock structure formed during back-arc basin deformation in the Andes of Tierra del Fuego. *Geological Society of America Bulletin*, **90**, 998–1012.

Camacho HH (1967) Las transgresiones del Cretácico superior y Terciario de la Argentina. *Revista de la Asociación Geológica Argentina*, **22**, 253–80.

Caminos R, Haller M, Lapido J, Lizuain O, Page A, Ramos VA (1981) Reconocimiento geológico de los Andes Fueguinos. Territorio Nacional de Tierra del Fuego. VIII Congreso Geológico Argentino, San Luis, Argentina. *Actas*, **3**, 759–86.

Capaccioni B, Didero M, Paletta C, Didero L (2005) Saline intrusion and refreshening in a multilayer coastal aquifer in the Catania Plain (Sicily, Southern Italy): dynamics of degradation processes according to the hydrochemical characteristics of groundwaters. *Journal Hydrology*, **307**, 1–16.

Cerredo ME, Tassone A, Coren F, Lodolo E, Lippai H (2000). Postorogenic, alkaline magmatism in the Fuegian Andes: the Hewhoepen intrusive (Tierra del Fuego Island). In: IX Congreso Geológico Chileno, Puerto Varas, Actas 2, Simposio Nacional 2, pp. 192–6.

Cerredo ME, Remesal MB, Tassone A, Lippai H (2005) The shoshonitic suite of Hewhoepen pluton, Tierra del Fuego, Argentina. In: XVI Congreso Geológico Argentino, La Plata. *Actas I*, **53**, 9–544.

Cerredo ME, Remesal MB, Tassone A, Menichetti M, Peroni JI (2007) *Ushuaia Pluton: Petrographic Facies and Geochemical Signature.* Tierra del Fuego Andes. International Geological Congress on the Southern Hemisfere (Geosur 2). Libro de Resúmenes, Santiago, Chile, 31 p.

Craig H (1963) Isotopic variations in meteoric waters. *Science*, **123**, 1702–3.

Dalziel IWD (1981) Back-arc extension in the southern Andes: a review and critical reappraisal. *Philosophical Transactions - Royal Society of London*, **300**, 319–35.

Dalziel IWD, Elliot DH (1973) The Scotia Arc and Antarctic margin. In: *The Ocean Basins and Margins vol. I: The South Atlantic* (eds Nairn AEM, Stehli FG), pp. 171–245. Plenum Press, New York.

Dalziel IWD, Brown RL (1989) Tectonic denudation of the Darwin metamorphic core complex in the Andes of Tierra del Fuego, southernmost Chile: implications for cordilleran orogenesis. *Geology*, **17**, 699–703.

Ellis AJ (1971) Magnesium ion concentrations in the presence of magnesium chlorite, calcite, carbon dioxide, quartz. *American Journal of Science*, **271**, 481–9.

Epstein S, Mayeda TK (1953) Variation of the $^{18}O/^{16}O$ ratio in natural waters. *Geochimica et Cosmochimica Acta*, **4**, 213–24. 1289 doi:10.1016/0016-7037(53)90051-9.

Fournier RO (1979) A revised equation for the Na/K geothermometer. *Geotherm. Res. Counc. Trans.*, **5**, 1–16.

Fournier RO (1991) Water geothermometers applied to geothermal energy. In Application of Geochemistry in Geothermal Reservoir Development. (F. D'Amore, coordinator), UNITAR, 37–69.

Giggenbach WF (1988) Geothermal solute equilibria. Derivation of Na-K-Mg-Ca geoindicators. *Geochimica et Cosmochimica Acta*, **52**, 2749–65.

González Guillot M, Escayola M, Acevedo R, Pimentel M, Seraphim G, Proenza J, Schalamuk I (2009) The Plutón Diorítico Moat: Mildly alkaline monzonitic magmatism in the Fuegian Andes of Argentina. *Journal of South American Earth Sciences*, **28**, 345–59.

Gupta H, Roy S (2007). *Geothermal Energy: An Alternative Resource for the 21st Century*. Elsevier, Amsterdam, the Netherlands, pp. 279.

Hemley JJ (1967) Aqueous Na/K ratios in the system K_2O-Na_2O-Al_2O_3-SiO_2-H_2O. Program, 1967 Ann. Meeting Geol. Soc. Amer. New Orleans, 94–5.

Katz HR (1972) Plate tectonics and orogenic belts in the southeast Pacific. *Nature*, **237**, 331–2.

Langelier WF, Ludwig HF (1942) Graphical method for indicating the mineral character of natural waters. *Journal of the American Water Works Association*, **34**, 335–52.

Lechler AR, Niemi NA (2011) The influence of snow sublimation on the isotopic composition of spring and surface waters in the southwestern United States: Implications for stable isotope–based paleoaltimetry and hydrologic studies. *Geological Society of America Bulletin*, **124**, 3–4. 318–334, doi: 10.1130/B30467.1.

Lodolo E, Menichetti M, Bartole R, Ben Avram Z, Tassone A, Lippai H (2003) Magallanes-Fagnano continental transform fault (Tierra del Fuego, southernmost South America). *Tectonics*, **22**, 6, 1076, doi:1029/2003TC0901500,2003.

Marini L, Ottonello G, Canepa M, Cipolli F (2000) Water-rock interaction in the Bisagno valley (Genoa, Italy): Application of an inverse approach to model spring water chemistry. *Geochimica et Cosmochimica Acta*, **64**, 2617–35.

Menichetti M, Tassone A (Eds.) (2007) GEOSUR2004: Mesozoic to Quaternary evolution of Tierra del Fuego and neighboring austral region I. *Geologica Acta*, **5**, 283–6. ISSN 1695-6133.

Menichetti M, Lodolo E, Tassone A (2008) Structural geology of the Fuegian Andes and Magallanes fold-and-thrust belt – Tierra del Fuego Island. *Geologica Acta*, **6**, 19–42.

Miranda FJ, Pesce AH (2000). Catalogue of thermal manifestations of Argentina Proceedings World Geothermal Congress 2000, Kyushu-Tohoku, Japan, May 28 - June 10, 2000, 1443–5.

Müller D, Groves DI (1993) Direct and indirect associations between potassic igneous rocks, shoshonites and gold-copper deposits. *Ore Geology Reviews*, **8**, 383–406.

Nelson E, Bruce B, Elthon D, Kammer D, Weaver S (1988) Regional lithologic variations in the Patagonian Batholith. *Journal of South American Earth Sciences*, **1**, 239–47.

Olivero EB, Martinioni DR (2001) A review of the geology of the Fuegian Andes. *Journal of South American Earth Sciences*, **14**, 175–88.

Orville PM (1963) Alkali ion exchange between vapor and feldspar phases. *American Journal of Science*, **261**, 201–37.

Pankhurst RJ, Riley TR, Fanning CM, Kelley SP (2000) Episodic silicic volcanism in Patagonia and the Antarctic Peninsula: Chronology of magmatism associated with the break-up of Gondwana. *Journal of Petrology*, **41**, 605–25.

Parkhurst DL (1995) User's guide to PHREEQC – A computer program for speciation, reaction-path, advective-transport, and inverse geochemical calculations: U.S. Geological Survey Water-Resources Investigations Report 95-4227, 143 p.

Peroni JI, Tassone A, Menichetti M, Cerredo ME (2009) Geophysical modeling and structure of Ushuaia Pluton, Fuegian Andes, Argentina. *Tectonophysics*, **476**, 6–449.

Pesce AH (1995) Argentina Country Update. Proceedings of the World Geothermal Congress 1995, Florence, Italy. Vol.1, 35–43,

Pesce AH (2005) Argentina Country Update. Proceedings of the World Geothermal Congress 2005. Antalya, Turkey, 12pp.

Pesce AH (2010) Argentina Country Update. Proceedings of the World Geothermal Congress 2010, Bali, Indonesia, 25–9.

Pesce AH, Pedro G (1995) Thermal model of the low enthalpy Rio Valdez geothermal field Tierra del Fuego, Argentina. Proceedings of the World Geothermal Congress. Florence, Italy, 1173–8.

Poage MA, Chamberlain CP (2001) Empirical relationships between elevation and the stable isotopic composition of precipitation and surface waters. Considerations for studies of paleoelevation change. *American Journal of Science*, **301**, 1–15.

Rabassa J, Heusser CJ, Coronato A (1989) Peat-bog accumulations rate in the Andes of Tierra del Fuego and Patagonia (Argentina and Chile) during the last 43000 years. *Pirineos*, **133**, 113–22.

Ridolfi F, Renzulli A, Cerredo ME, Oberti R, Baiocchi M, Bellatreccia F, Della Ventura G, Menichetti M, Tassone A (2010) Amphibole megacrysts of the Cerro Jeu-Jepén Pluton: new constraints on magma source and evolution (Fuegian Andes, Argentina). In: Geosur, 22–23 November 2010, Mar del Plata, Argentina extended abstracts, 80–3.

Rossello EA, Haring CW, Cardinali G, Suarez F, Laffitte GA, Nevistic AV (2008) Hydrocarbons and petroleum geology of Tierra del Fuego, Argentina. *Geologica Acta*, **6**, 69–83.

Shapiro AM, Hsieh PA (1998) How good are the estimates of transmissivity from slug tests in fractured rocks? *Ground Water*, **36**, 37–48.

Tassone A, Lippai H, Lodolo E, Menichetti M, Comba A, Hormaechea JL, Vilas JF (2005) A geological and geophysical crustal section across the Magallanes-Fagnano fault in Tierra del Fuego. *Journal of South American Earth Sciences*, **19**, 99–109.

Truesdell AH, Hulston JR (1980) Isotopic evidence on environments of geothermal systems. In: *Handbook of Environmental Isotope Geochemistry* (eds Fritz P, Fontes JCh), vol 1, pp., 179–226. The Terrestrial Environment, A, Elsevier, Amsterdam, the Netherlands.

GEOFLUIDS

Volume 13, Number 1, February 2013
ISSN 1468-8115

CONTENTS

WILEY Blackwell

Geofluids* is abstracted/indexed in *Chemical Abstracts

This journal is available online at Wiley Online Library. Visit onlinelibrary.wiley.com to search the articles and register for table of contents and e-mail alerts.